

# CYTOTOXIC EFFECT OF ASPARAGINASE PRODUCE FROM *E. COLI* AND CONJUGATED WITH ZNO NANOPARTICLES ON CANCER CELL LINES

Zahraa H. H.

H. A. Rasheed

Researcher

Lecturer

<sup>1</sup>Dept. Biotech. Sci. Col., University of Baghdad, Baghdad Iraq

Szo3168@gmail.com

hala.aljendeel@gmail.com

## ABSTRACT

This study was aimed to examine the anticancer activity of fabricated ZnONPs- L-ASNase conjugate against cancer and normal cell lines. Total of 127 bacterial isolates were taken from clinical and environmental samples then identified as *E. coli*. In this work, 88 isolates were identified as *E. coli*. L-asparaginase produced from *E. coli* were screened, clinical Isolates of *E. coli* from urine sample have the potential to produce asparaginase that is responsible for cytotoxicity, the optimal culture conditions for the development of the enzyme L-asparaginase were determined to be 37°C and pH8. Nitrogen source concentrations at 0.9gm/ml were discovered to maximize enzyme production. L-asparaginase then purified by two steps that include ion exchange column and gel filtration. Purification and recovery percentage for L-ASNase was 6.21%, 10.34% respectively. Effective conjugation was approved by UV-visible spectroscopy. ZnO nanoparticles exhibit absorbance peaks approximately 200-300 nm. XRD analysis confirmed the crystallite size of the ZnO nanoparticles was observed to be 18.4 nm. The activity of L-ASNase in the ZnONPs-L-ASNase was detected by a direct nesslerization method and the findings showed a substantial increase L-ASNase specific activity within the conjugate of ZnONPs-L-ASNase in comparison to its free state. The ZnONPs-L-ASNase conjugate showed the greatest and most substantial cytotoxic action against A375 with survival rate at 400 µg /mL about 45.8± 2.3. The IC50 value of 44.69 µg/ mL of ZnONPs- L-ASNase was calculated for A375 cells. In comparison, all substances exhibited weak to moderate cytotoxicity when tested against the normal cell line WRL-68. The ZnONPs-L-ASNase combination therapy resulted in a higher cytotoxic effect. This action could be attributed to the synergetic effects of both L-ASNase and the conjugated molecules ZnONPs.

Keywords: purification, the ZnONPs-L-ASNase conjugate, anticancer activity

زهراء ورشيد

مجلة العلوم الزراعية العراقية - 2023: 54(6): 1664-1678

التأثير السمي لل asparaginase المنتج من *E. coli* و المرتبط بجزيئات ال ZnO النانوية على سمية الخلايا السرطانية

حلا عبد الكريم رشيد

زهراء حسن حيدر

المدرس

الباحثة

قسم التقنيات الاحيائية، كلية العلوم، جامعة بغداد، بغداد، العراق

## المستخلص

هدفت هذه الدراسة إلى فحص النشاط المضاد للسرطان لمقارنة ZnONPs- L-ASNase المصنع ضد السرطان وخطوط الخلايا الطبيعية. تم أخذ ما مجموعه 127 عزلة بكتيرية من العينات السريرية والبيئية ثم فحصها وتحديدتها على أنها الإشريشيا القولونية. في هذا العمل ، تم تحديد 88 عزلة على أنها الإشريشيا القولونية، تم غربلة الأسباراجينيز العزلات السريرية للإشريكية القولونية من عينة البول لديها القدرة على إنتاج الأسباراجينيز المسؤول عن السمية الخلوية. تم تحديد الظروف المثلى لإنتاج إنزيم L-asparaginase لتكون 37 درجة مئوية والاس الهيدروجيني 8. تم اكتشاف تركيز مصدر النتروجين عند 0.9 جم / مل لزيادة إنتاج الإنزيم المنتج من الإشريكية القولونية ثم تمت تنقيته بخطوتين تشملان عمود التبادل الأيوني والترشيح الهلامي. نسبة التنقية والاسترداد ل L-ASNase كانت 6.21% ، 10.34% على التوالي. بدأ تحضير اتحاد ZnONPs- L-ASNase أولاً عن طريق تخليق ZnONPs بالطريقة الكيميائية. تم تأكيد الاقتران الناجح بواسطة التحليل الطيف المرئي للأشعة فوق البنفسجية. تظهر جزيئات ZnO النانوية قمم امتصاص في حدود 200-300 نانومتر. أكد تحليل XRD أن الحجم البلوري للجسيمات النانوية ZnO كان 18.4 نانومتر. تم الكشف عن نشاط L-ASNase في ZnONPs-L-ASNase بواسطة طريقة nesslerization مباشرة وأظهرت النتائج زيادة كبيرة في نشاط معين ل L-ASNase داخل اتحاد ZnONPs-L-ASNase عند مقارنته بحالته الحرة. أظهر اتحاد ZnONPs-L-ASNase أقوى نشاط سام للخلايا وأعلى بكثير ضد خلايا A375 مع معدل بقاء عند 400 ميكروغرام / مل حوالي 45.8 ± 2.3. تم حساب قيمة IC50 البالغة 44.69 ميكروغرام / مل من ZnONPs- L-ASNase لخلايا A375. على النقيض من ذلك ، أظهرت جميع المركبات سمية خلوية ضعيفة ومتوسطة على خط الخلايا الطبيعي WRL-68. نتج عن العلاج المركب ZnONPs-L-ASNase تأثير سام للخلايا أعلى. يمكن أن يعزى هذا الإجراء إلى التأثيرات التآزرية لكل من L-ASNase والجزيئات المقترنة ZnONPs

الكلمات المفتاحية: التنقية، الأسباراجينيز المربوط مع اوكسيد الزنك النانوي، الفعالية المضادة للسرطان.

## INTRODUCTION

L-asparaginase is a widely distributed enzyme that is present in bacteria, fungi, yeast and plants. It stimulated the degradation of the amide group in L-asparagine to result of ammonia and aspartate (12, 17). L-asparaginase has been shown in numerous studies to have anti-leukemic action (13, 27). L-asparaginase is currently a serious medicine in treatment leukemia of the lymphoblastic kind in children all over the world. L-asparaginase is sold under the product names oncaspar, kidrolase, elspar, and ERWINASE (16). L-asparaginase was thought to have anticancer effect because of absence of L-asparagine synthetase in most tumors, exogenous input of L-asparagine is required from circulating pools. Normal cells, alternatively, produce L-asparagine in adequate quantities for use aspartic acid and glutamine to generate sufficient amounts of L-asparagine for protein synthesis within cells, or they can take up L-asparagine synthetase from the cell's environment and use that instead. A neoplastic protein synthesis inhibitor, L-asparaginase, transforms circulating asparagine to L-aspartate and ammonia. consequently, the most popular treatment for this illness is to deliver L-asparaginase intravenously to reduce the level of L-asparagine in blood and destroy its supply to specially attack the necrotic or cancerous cells (31). Microbial supplies are especially abundant and accessible for production L-asparaginase due to their ease of cultivation and ability to provide separated and purified compounds as well as making industrial scale production possible (30). The most frequently used microorganisms in the manufacture of L-asparaginase were *Escherichia coli*, *Streptomyces albidoflavus*, *Bacillus sp.* and *actinomyces* from the *rhizosphere* of medical plants (22). L-asparaginase produced by *Erwinia chrysanthemi* and *E.coli* inhibits tumor cell activity perfectly. They have been used clinically in treatment Hodgkin's infection, reticule-sarcoma, chronic lymphocytic leukemia, acute myelomonocytic leukemia, lymphosarcoma, acute myelocytic leukemia and Melan sarcoma (13). *Escherichia coli* is a rod-shaped gram-negative bacteria observed in warm-blooded creatures' lower intestines

(endothems). Humans are at risk of acute food poisoning, septicaemia meningitis, and urinary infections caused by pathogenic *E. coli* strains (30). It is responsible for 80% of community acquired UTI (3). Urinary tract infection (UTI) means the colonization and infections by one or more urinary tract parts (18, 21). *Escherichia coli* is the most utilized expression system for the creation of recombinant proteins. All these advantages enable *E. coli* to produce recombinant proteins in a quick, high-yielding, and cost-effective manner (6). For several all-treatment protocols, asparaginase obtained from *E.coli* is believed first-line treatment (10). The negative effects of intravenous injection of L-asparaginase have emphasized the need for new cancer treatment delivery systems. When a medicine is being delivered to a cancer patient, nanoparticles are how it will get there (24). A nano-bio-composite comprising zinc oxide nanoparticles and L-asparaginase was made by *E.coli* in this experiment. According to research, zinc nanoparticles have anti-cancerous and anti-microbial properties (5). Zinc oxide possesses superior electrostatic properties, enabling it to have several charges on its surfaces at both acid and basic pH values. To internalize nanoparticles into cancer cells, this characteristic can be employed to conjugate therapeutic compounds and to internalize nanoparticles with a negatively charged surface. As a photodynamic agent, zinc oxide nanoparticles can also cause cell death when they are illuminated (21). With these characteristics, zinc oxide nanoparticles are a good choice for medication delivery. When medicinal drugs are combined with zinc oxide nanoparticles, better outcomes are obtained than when using any other nanoparticle. L-asparaginase was conjugated to zinc oxide nanoparticles, known as metalloproteins, and its lethal influence on cancer cells was examined in this study. The cytotoxic effect was investigated using skin cancer cell line and normal cell line. Accordingly, the purpose of this research was to find isolates potential of producing a large amount of L-asparaginase and to assess the anticancer action of purified L-ASNase linked with zinc oxide nanoparticles against a cancer cell line.

**MATERIALS AND METHOD****Table 1. Chemical & Biological materials used in this study**

Material	Company / Origins
Meat extract	Himedia / India
Phenol red	Buchs SG/ Switzerland
Sodium hydroxide	Sigma/ USA
Ammonium sulfate	BDH / Englan
K <sub>2</sub> HPO <sub>4</sub>	Fluck / Switzerland
Yeast extract	Himedia / India
Hydrochloric acid	BDH / Englan

**Collection of samples**

Between October 2020 and January 2021, a total of 127 samples were collected, including 109 samples of urine and feces and 18 samples of sewage (collected from various places). Each one of the clinical samples gathered from patients (Male ages ranged from 5 to 50 years) at two hospitals in the Baghdad district: the city of medicine hospital and the National Center of Teaching Laboratories. Transport media are used to collect samples, which are subsequently chilled in an icebox on the way to the lab. The samples were cultured for 24 hr. at 37°C in nutrient broth.

**Bacterial identification**

All samples were identified by morphology, biochemical analysis, and the VITEK-2 System (15).

**Qualitative screening for asparaginase production:** *Escherichia coli* were examined for L-asparaginase production. rapid plate assay with modified agar plate (containing nutrient agar, 1% L-asparagine, and 2.5% phenol red along with pH 7) was used to measure the isolates ability for production of L-asparaginase enzyme.

**L-asparaginase production**

For L-asparaginase production, 250 mL flask was filled with yeast extract media, which prepared by adding 0.6% yeast extract and 0.2 % Tryptone soy broth and (10.75g) NaHPO<sub>4</sub>, (3.55g) KH<sub>2</sub>PO<sub>4</sub>, (0.025g) MgSO<sub>4</sub>, (0.0027g) FeSO<sub>4</sub>.7H<sub>2</sub>O, (0.0025g) MnCL<sub>2</sub>.4H<sub>2</sub>O and (0.015g) CaCL<sub>2</sub>.6H<sub>2</sub>O. After that, inoculating production medium (100ml) with overnight bacterium broth (2ml) (OD > 0.5), then incubated at 37°C for 24 hr. at 120 rpm. The bacterial pellets were collected by centrifugation after growing on production media. After removing the supernatant, the particle was washed twice with sterilized DW. The pelleted cells were washed with distilled

water and sonicated (30-sec sonication, 1min stop, ten cycles). After that, the supernatant was centrifuged at 8000 rpm for 15 minutes then processed in a freezer for enzyme assay and purification.

**L-asparaginase assay**

According to (25), asparaginase was measured using the Nesslerization process, this is depend on the transformation of L-asparagine into ammonia and L-aspartate and has an absorption limit at 436 nm. The activity of asparaginase from *E. coli* extracts was calculated by mixing 0.25 ml of crude enzyme with (200 mM) of L-asparagine (1ml) as prepared in, after that 1ml of KH<sub>2</sub>PO<sub>4</sub> (0.05M, pH 8.0) was included, gently combined, and incubated at 37°C for 30 min. in a water bath. After incubation, the reaction was ended by adding (1.5M) trichloroacetic acid (TCA) (0.5 ml) to the reaction mixture, then centrifuged for 10 min at 8000 rpm. The activity of enzyme in the supernatant was measured, and the ammonia concentration in the clear supernatant was determined using direct Nesslerization process. Each sample's ammonia concentration was calculated by combining 3 mL distilled water, 0.5 mL Nessler reagent and 0.5 mL supernatant in a volumetric flask. The solution had been mixed vigorously. At 436 nm, the absorbance was measured. 3.5 mL distilled water + 0.5 mL Nessler's reagent was used to render the blank. Under experimental conditions, one unit of L-asparaginase (IU) is specified as the quantity of enzyme that releases 1 mol of ammonium per minutes. The equation used to quantify asparaginase activity according to (14).

**Optimization for crude L-asparaginase production from *E. Coli* ZH30:** The influence of various culture requirements L-asparaginase production was examined. Numerous regulating parameters including nitrogen concentration, pH value and temperature were studied.

**Effect of Ph:** Using varied pH (7, 8, and 8.5) the influence of pH on the production of L-asparaginase was established. After then, the enzyme specific activity was calculated. protein concentrations were established by Bradford (7).

**Effect of temperature:** The production media was inoculated and incubated at various

temperatures (25, 30, 37, and 40°C) to identify the optimum temperature for L-asparaginase production. After then, the enzyme activity and protein conc. were estimated.

#### **Effect of nitrogen source concentration**

Using varied ratios of nitrogen source (yeast extract) (0.3, 0.6, and 0.9g/ml). The influence of nitrogen source concentrations on the production of L-asparaginase was established. After then, the enzyme activity and protein concentrations were estimated.

**Asparaginase purification using ion exchange chromatography:** According to Whitaker (32), ion exchange chromatography was used for L-asparaginase purification. A CMC-column 9.9×1.5cm (radius×length) was adjusted and washed along with 0.1M of potassium phosphate buffer (PH 8) many times. The CMC column was refilled with 7.2 ml of concentrated enzyme. The samples were accumulated at a flow rate of 3 ml/fraction during the wash phases. With 0.1 M Tris-HCl buffer pH8 and NaCl in a linear gradient from 0.1 to 1 M, we separated the bound proteins and evaluated the absorbance of all fractions at 280 nm. The peaks were collected and tested for asparaginase activity.

**Asparaginase purification by SephacryleS-200:** The Sephacryle S-200 gel column 0.5×32 cm (radius×length) was prepared according to the instructions provided by Pharmacia Fine Chemicals. The column was washed and equilibrated with 0.1M potassium phosphate buffer (pH 8) before being loaded with 12 ml of concentrated enzyme purified by CMC column. The elution was carried out at a flow rate of roughly 3 ml/fraction using potassium phosphate buffer, all the samples were analyzed using a UV spectrophotometer set to 280 nm, the peaks were tested for enzyme activity.

#### **Protein concentration measurement**

The concentration of proteins was measured using the Bradford technique.

#### **Preparation of Zinc Oxide nanoparticles**

The nanoparticles of zinc oxide were made using chemical method from zinc chloride that carried out with (9) various modifications. Sodium Hydroxide (1.0 M) was melted in 100 mL D.W, the resultant solution was heated to the required reaction temperature (90°C) with steady stirring. 6.8 g of ZnCl<sub>2</sub> (0.5 M) was

suspended in 100 ml distilled water after reaching the required temperature, and the resultant solution was dropped into the NaOH solution drop by drop (dripping 60 min). When ZnCl<sub>2</sub> is dripped into an aqueous alkaline solution, ZnO precipitates almost immediately, and the color changes from translucent to white. After dripping is complete, the solution is stirred for one hour, maintain the proper temperature (90°C). The particles were separated from the dispersion of supernatant. The supernatant was separated, the suspension was rinsed five times with distilled water to ensure that all NaCl was removed. The concentrated to washing solution dilution ratio was about 1:10 each time. Ethanol absolute was used to peptize the purified particles in an ultrasonic bath for 10 minutes at 27°C. To disrupt micro-agglomerates and release nano units from bulk suspensions, the peptization process is required. The particles were subsequently collected by centrifugation for 15 minutes at 8,000 rpm. For several hours, accumulated particles were dried in vacuum oven at a maximum temperature of 70°C.

**Preparation ZnONPs and L-ASNase conjugate:** ZnONPs (1mg/ml) were prepared in different concentrations by dissolving 0.002g of ZnO in 2ml de-ionized water and made various concentration from ZnO (200, 100, 75, 50, 25, 12.5µg/ml). ZnONPs-L-ASNase conjugate were prepared by mixing 4ml of L-ASNase (1.6mg/ml) and 4 ml of each concentration of ZnO. The mixture of each concentration was incubated at 4°C for 30min under gentle stirring and leave it overnight at 4°C. Following that, the solutions were precipitation using a centrifuges (6000 rpm for 30 minutes each round at 4°C). After removing the supernatant, the pellet was gathered as the final product.

**Characterization of ZnONanoparticles and (ZnONPs-L-ASNase) Conjugate:** The synthesis of ZnO NPs were characterized using UV-Vis Absorption Spectrophotometry, Fourier Transform Infrared Spectroscopy (FTIR), Atomic Force Microscope (AFM), X-Ray Diffraction (XRD) and Zeta Potential.

**Cytotoxic effect of purified L-ASNase, ZnO NPs, ZnO NPs-L-ASNase on A375:** The possible cytotoxic effects of L-ASNase, ZnO, and ZnO-L-ASNase (conjugated) were

investigated using this in vitro approach. They were prepared in various concentrations and their cytotoxicity was tested on tumor cell lines (A375) and the WRL 68 cell line as a control cell line (28).

## RESULTS AND DISCUSSION

**Primary screening (qualitative) of isolates for L-asparaginase production:** From the total of 88 bacterial isolates that belonged to *E.coli*, only 66 strains provide positive results for the production of L-ASNase besides 22 isolates revealed negative test for L-ASNase

after cultured in modified nutrient agar for detecting enzyme production in which asparagine served as a substrate for the enzyme. The presence of red color around colonies of organisms (as shown in figure 1), which is caused by the deamination or release of ammonia from asparagine, whereas used to identify the Asparaginase positive colonies. The synthesis of ammonia raises the pH of the medium, turning it reddish or pinkish purple in appearance.

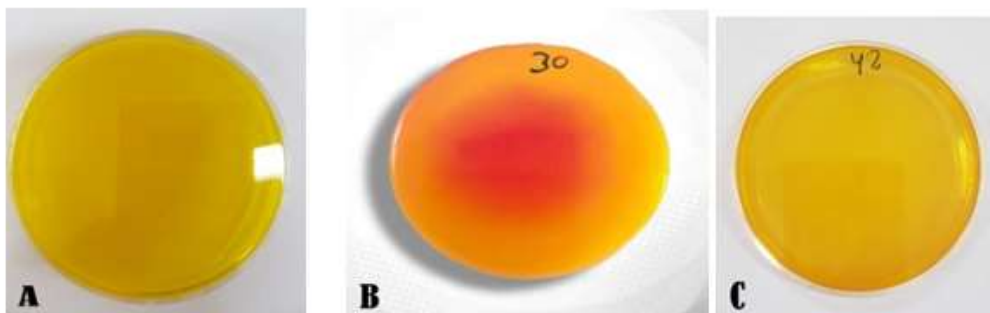


**Figure 1. Asparaginase production screening test (qualitative assay). A- represent a control dish, B- Asparaginase positive strain, C-Asparaginase negative strain.**

**Secondary screening of isolate for L-ASNase production:** In qualitative screening, fourteen *E. coli* isolates with the highest biodegradation ability were screened using production media supplemented with yeast extract. Analyses were performed utilizing the Nesslerization procedure, this is based upon the transformation of L-asparagine to ammonia and L-aspartate with an absorption limit of 436nm (19). Using these results, we can better identify and select asparaginase-producing bacteria by comparing the activity of intracellular vs external asparaginase enzymes. The results indicate that the internal asparaginase enzyme is more active against asparagine than the extracellular asparaginase enzyme. The *E.coli* ZH 30 strain isolated from a clinical urine sample showed the highest enzymatic activity about 4.5 U/ml, whereas the other isolates had asparaginase activity varying from 0.2 to 1.25U/ml. Based on these findings, active *E. coli* ZH 30 isolate was selected for use in the subsequent research.

**Optimal conditions for crude asparaginase production:** After screening the enzyme production from *E.coli* strain, the optimal conditions for asparaginase production were studied for ZH 30.

**Effect of pH:** The effect of pH on the production of asparaginase produced by *E.coli* ZH30 was studied. The results in Figure (2) show revealed that the optimum pH value of the production media is 8.0 with highest enzyme specific activity about 2.2U/mg. The Asparaginase produced by *E. coli* is reported to have the highest activity at alkaline pH, which may be due to the balance between L-aspartate and aspartic acid. Aspartic acid has a higher affinity for the active site of the enzyme at acidic pH (12).

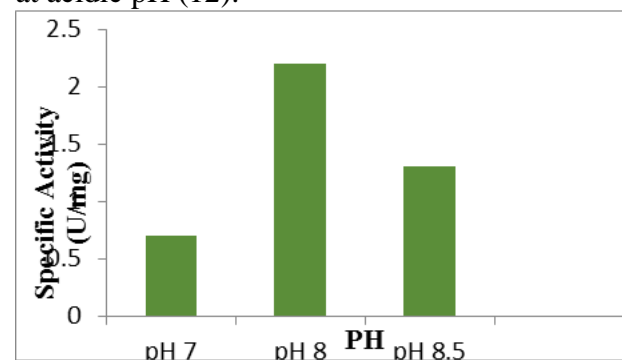


**Figure 2. Effect of pH on asparaginase production extracted from *E. coli* ZH30, incubated at 37 ° C for 24hr**

**Effect of temperature on enzyme production:** Various temperatures (25, 30, 37, and 40°C) were tested to identify the best incubation temperature to produce

asparaginase isolated from *E.coli* ZH30. This temperature range was shown to be the most conducive to enzyme production. The greatest specific activity of asparaginase was found at 37°C with enzyme activity about 2.2U/mg, while the enzyme specific activity was reduced, when the incubation temperature raised or lowered above or below the optimal temperature as shows in figure (3). The maximal specific activity of asparaginase for most species was discovered to be 37°C (2). Temperature affects the rate of biochemical processes by promoting or inhibiting enzyme synthesis (29).

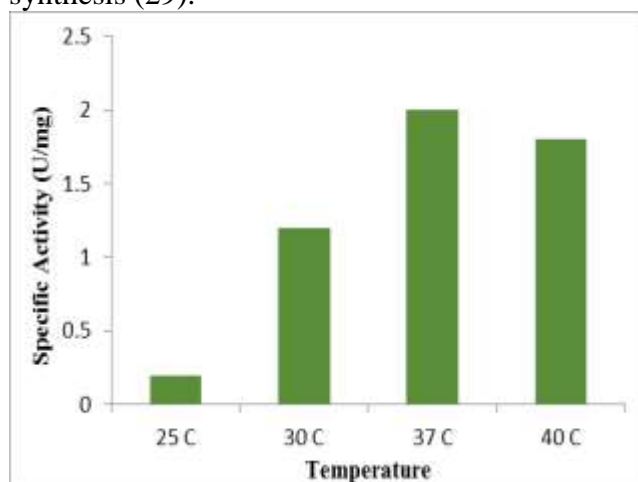


**Figure 3. The influence of temperature on the production of asparaginase isolated from *E.coli* ZH30**

**The influence of nitrogen source concentration:** The results of Figure (4) showed that when the concentration of yeast extract (nitrogen source) increases, the specific activity of asparaginase gradually increases. When the yeast extract concentration is (0.9 g/ml), the L-asparaginase specific activity is the highest and, at this concentration, the L-asparaginase specific activity is (3.8U/mg). The optimal yeast extract concentration for L-asparaginase production was determined using three concentrations of enzyme-nitrogen source (yeast extract) (0.3, 0.6, 0.9 g/ml). At this concentration, the L-asparaginase specific activity was (3.8U/ mg) while the specific activity of L-asparaginase using yeast extract

at concentrations 0.3 and 0.6g/ml were 2.3U/mg and 2.5 U/mg, respectively. This yeast extract with a concentration of (0.9 g/ml) was considered the optimum concentration for L-asparaginase production.

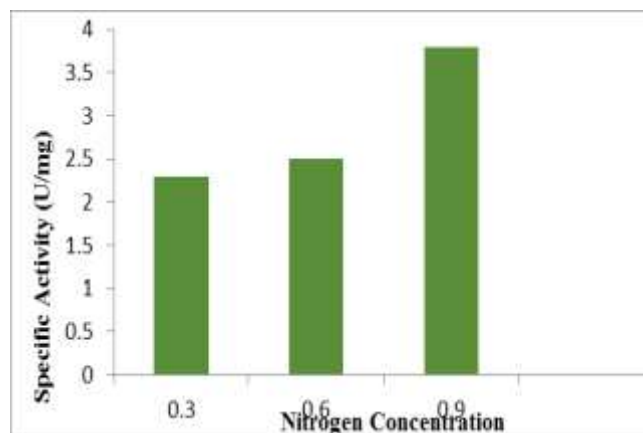


**Figure 4. Influence of nitrogen concentration (meat extract) on the production of L-asparaginase extracted from *E. coli* ZH30, incubated at 37°C for 24 hr**

**Ion exchange chromatography Purification of L-ASNase:** The first step in the purification of L-ASNase was by Ion exchange method, L-ASNase was applied to Carboxymethyl cellulose column (CMC). The results were shown in figure (5) revealed the presence of four peaks of protein and one peak of L-ASNase in the wash step. In the Elution step the result were shown many protein peaks, and no enzyme activity. The percent of purification fold and yield of L-ASNase in the peak was (1.32%) and (80.9%), respectively that illustrated in (table 2). The choice of ion exchanger depends on the net charge of protein (L-asparaginase). according to the findings, L-asparaginase activity was shown to be optimal at pH8 in this investigation, and the pI of this enzyme (pI=4.5-5) as described by Chagaz and Sodek(8), it could be concluded that asparaginase extracted from *E.coli* have negative charge.

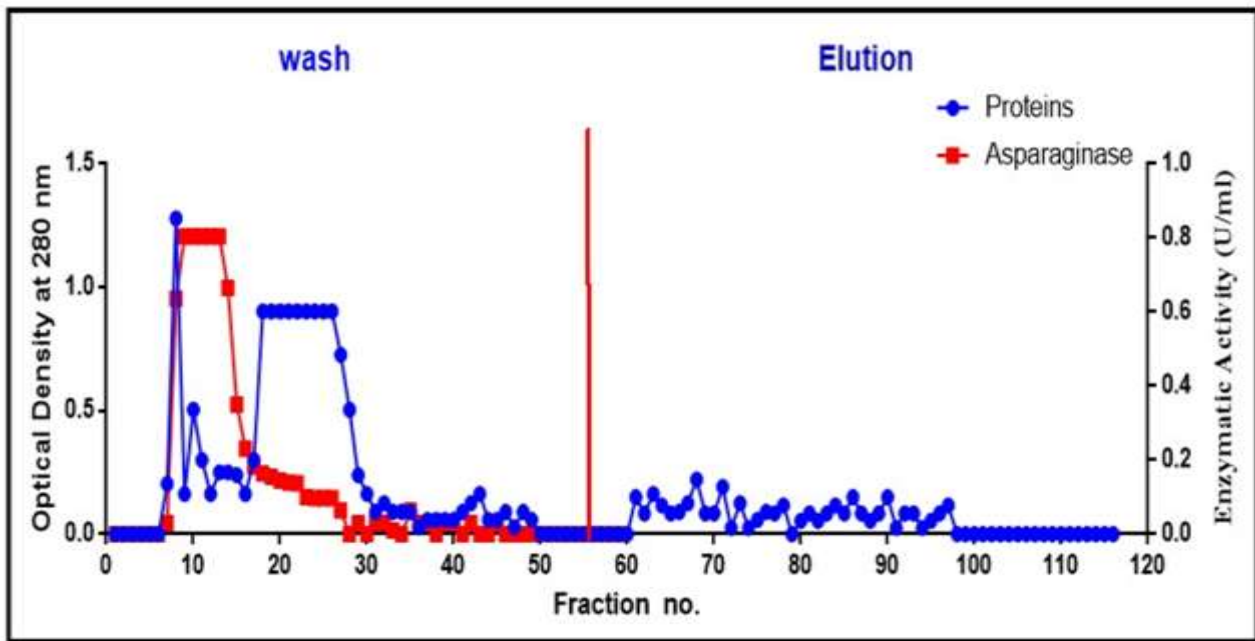


Figure 5. Ion exchange chromatography using a CMC column (9.9× 1.5 cm) (radius×length) to purify L-asparaginase produced by *E. coli* ZH30 at a flow rate of 20 ml/hr

**Purification of L-ASNase using Sephacryl S-200:** The second step in the purification of L-ASNase was by gel filtration chromatography method. The fractions that contain the L-ASNase were collected and applied to Sephacryl S-200. The elution curves achieved in these methods illustrated in Figure (6), which revealed two protein peak and two peaks contained the L-ASNase, the fold purification and recovery of asparaginase in the first peak was 1.91 and 23.87%, respectively. while the second peak exhibited

fold purification and recovery around 6.21 and 10.34%, respectively that illustrated in (table 2). Protein peaks were established by estimating optical density at 280 nm utilizing UV-VIS spectrophotometer. In contrast, the L-asparaginase from *Enterobacter aerogenes* was purified using Sephacryl S-100 as the separating medium in gel filtration, and then ultra filtration with the specific activity of 55 IU/mg of protein and a recovery rate of 54%, a ten-fold increase in purity is achieved with this method (20).

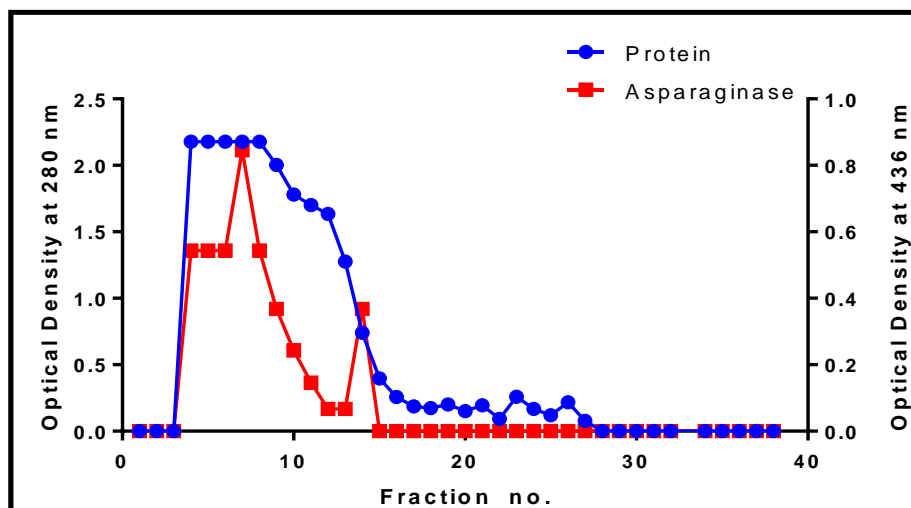


Figure 6. Chromatography gel filtration using Sephacryl S-200 column (32×0.5 cm) (radius×length) to purify L-asparaginase produced by *E. coli* ZH30 at a flow rate of 20 ml/hr

**Table2. purification table of L-asparaginase from *E. coli* ZH30**

Purifications Stage	volume (ml)	Asparaginase (U/ml)	Protein Conc. (mg / ml)	Specific activity (u/mg)	Asparaginase Total Activity (U)	Fold Purification	Recovery%
Concentrated supernatant	7.2	8.3	2.4	3.46	59.76	1	100
Ion Exchange by CMC	12.4	3.9	0.854	4.57	48.36	1.32	80.9
Gel Filtration by Sephacryle S-200 first peak	15	0.95	0.109	8.72	14.26	1.91	23.87
Gel filtration Sephacryle S-200 Second peak	3	2.06	0.038	54.21	6.18	6.21	10.34

**Preparation of Zinc Oxide Nanoparticles**

ZnO nanoparticles were manufactured using the chemical precipitation process, as described in material and method. ZnO nanoparticles seem white in appearance

**Conjugation of zinc oxide nanoparticles with L-ASNase:**

The result shows a significant rise in the specific activity of L-ASNase in the conjugated state compared to its free form, with a calculated specific activity of L ASNase (1U/mg) which is increased to (2.9 U/ mg) when conjugated with ZnO NPs at a concentration of 25 (µg/ml) as shown in table 3. These results show good agreement with those of (24), who reported increased L-ASNase specific activity in the presence of ZnO NPs compared to crude L-ASNase. The proposed chemo synthesized ZnO nanoparticles showed considerable stability

and best conjugation to L-ASNase at concentration (27) (µg/ml) depending on the highest specific activity of the conjugated L-ASNase with ZnONPs, then UV–visible spectroscopy was used to confirm the effective conjugation as revealed in Figure (7).

**Table 2. the conjugated concentrations of ZnO-L-ASNase with their specific activity**

specific activity ZnO Concentration(µg/ml) after conjunction	Specific Activity U/mg
200	1.7 U/mg
100	2.2 U/mg
75	2.5 U/mg
50	1.9 U/mg
25	2.9 U/mg
12.5	1.7 U/mg

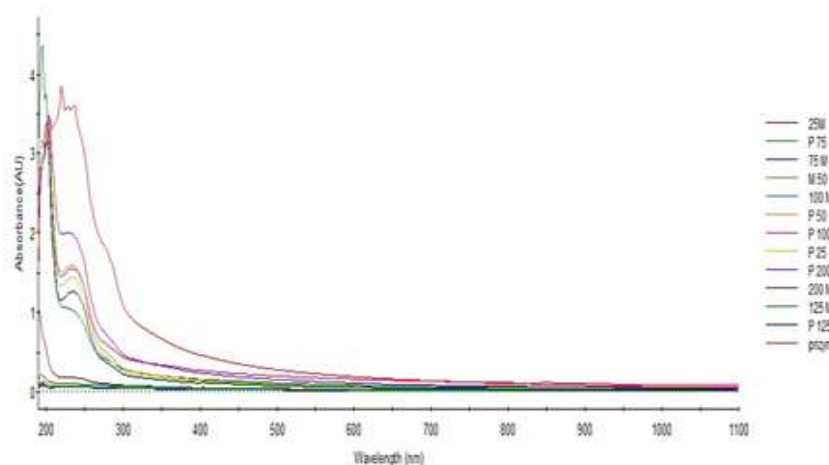


**Figure7. The UV-VIS absorption spectra of different concentrations of ZnONPs and ZnO-L-ASNase(conjugated), the M refer to non-conjugated ZnONPs, and the P refers to the conjugated ZnO-L-ASNase**



### Characterization of ZnO Nanoparticles and (ZnONPs-L-ASNase) Conjugate:

The synthesis of ZnONPs and ZnONPs-L-ASNase conjugate were characterized by UV-Vis's spectrum, FTIR, XRD, AFM, Zeta Potential.

### Spectrophotometry of UV-Visible Absorption:

UV-visible spectroscopy was used to confirm successful conjugation. As show in the Figure (8). ZnO nanoparticles exhibit absorbance peaks in range of 200-300

nm, which can be attributed to the plasm on resonance of Zinc oxide nanoparticles. The absorption spectrum shifts toward the end depending on the particle size, shape, surrounding medium, and aggregation state. The UV-visible absorption peak strength has been shown to be proportional to nanoparticle particle size, according to research. The absorption peak moves toward a shorter wavelength as particle size decreases

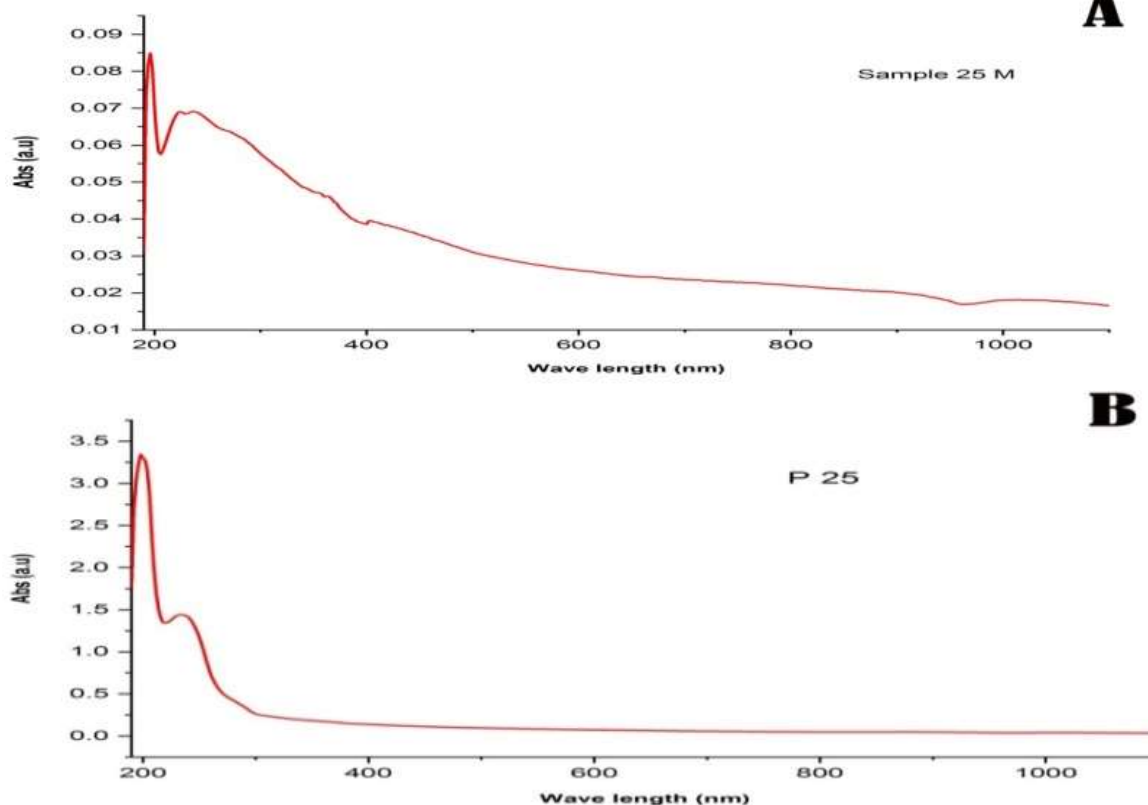


**Figure 8. The UV-vis absorption spectra (A) represent the ZnONPs concentration, (B) represent ZnONPs-L-ASNase conjugate**

**Fourier transform infrared spectroscopy (FT-IR):** FTIR spectroscopy was applied to determine the chemical surface area and the ends of the functional groups of ZnONPs ,ZnO NPs-LASNase (Figure 9 A and B). The spectrum shows an average of 20 scans in the range from 4000 to 400  $\text{cm}^{-1}$  with a resolution of 4  $\text{cm}^{-1}$ . The peaks at 3431.13,  $\text{cm}^{-1}$  and 3409.19 reflected a functional group O-H together with a H-bound data vibration that was strong in strength. Also noticed were absorption peaks ranging from 400 to 4000  $\text{cm}^{-1}$ , which corresponded to the hydroxyl and carboxylate in materials. The stretching mode of the O-H hydroxyl group is responsible for the broadband around 3120  $\text{cm}^{-1}$  (1). The peak at 1618.17 reflected a functional group C=C that

was strong in strength. The stretching vibrations of C=C and C=O, as well as the exocyclic -NH<sub>2</sub> bases, were discovered to correlate to the first (1600-1750  $\text{cm}^{-1}$ ); these findings were shown to agree with (13). Furthermore, the series of absorption peaks ranging from 400 to 4000  $\text{cm}^{-1}$  which correspond to hydroxyl and carboxylate in materials could be noted. The next region (1500-1650) was dominated by both methyl pyrrole modes, which had previously been discovered by (23). The ZnO NPs and ZnONPs-L-ASNase showed common characteristic peaks, while some differences had existed because of a slight chemical interaction of L-ASNase inside the ZnONPs-L-ASNase. New peaks generated in FT-IR

spectra of ZnO NPs-L-ASNase that were not present in ZnO NPs spectra, as shown in Figure 3-18B; the strong NH group with a peak at 3429.20 cm<sup>-1</sup> indicated the existence

of L-ASNase on the ZnO NPs. As a result, the FT-IR data revealed that the procedure of functionalization with L-ASNase had no effect on the primary properties of the ZnO NPs.

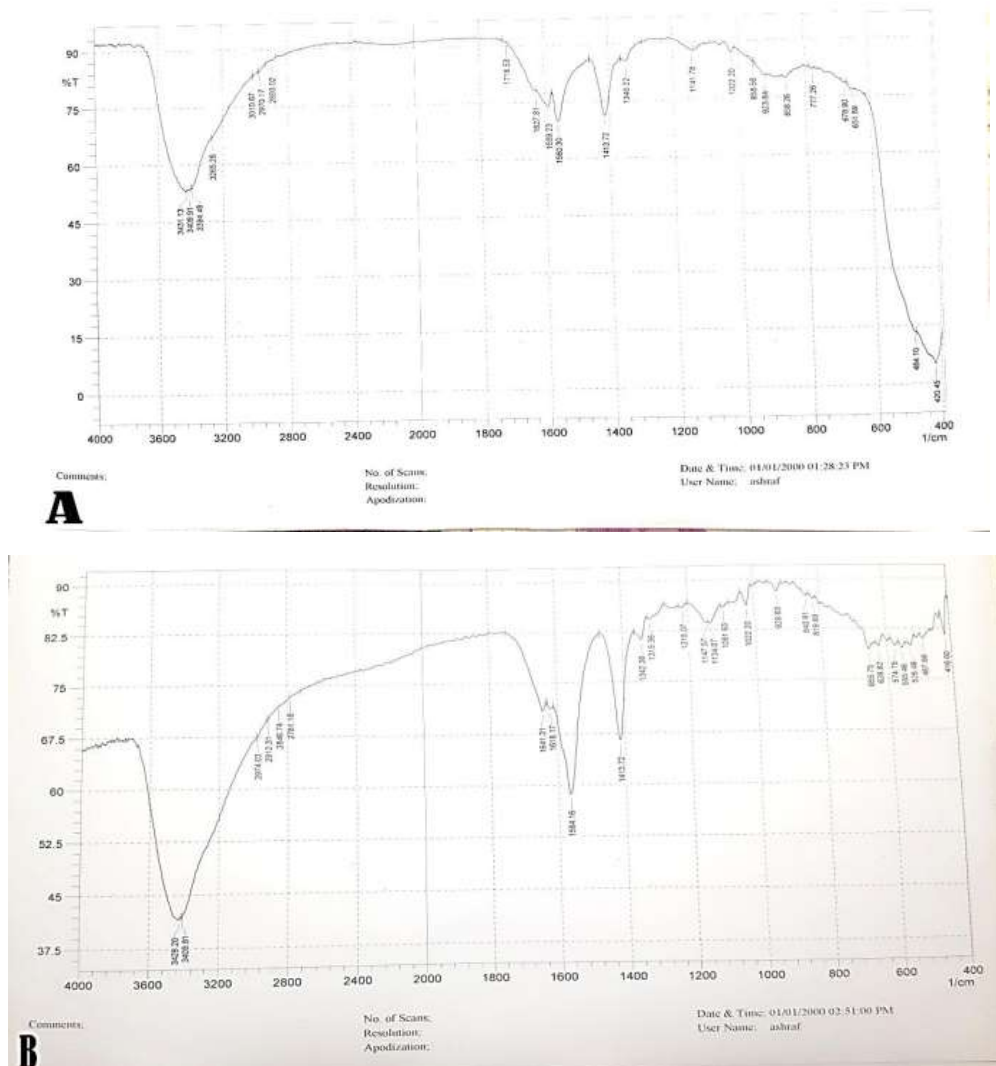


**Figure 9. FT-IR analysis of (A) ZnO NPs and (B) ZnO NPs-L-ASNase. Experiments performed at room temperature**

**X-Ray Diffraction (XRD):** The X-ray diffraction design of ZnO nano powder is revealed in Figure (10). The XRD peaks show a distinct line widening, indicating that the material is composed of nanoscale particles. We were able to determine peak intensity, location, and width (FWHM) from this XRD pattern analysis. These six diffraction peaks (31.84°, 34.52°, 36.33°, 47.63°, 56.71°, 62.96°, and 69.18°) have been identified as ZnO hexagonal wurtzite. Furthermore, the lack of any XRD peaks other than ZnO peaks suggests that the produced nano powder was free of contaminants. There were no recognizable peaks of contamination in

this sample. The peaks at scattering angles of 31.64°, 34.85°, 36.65°, 46.1°, 57.12°, 63.2°, 68.9° which relates to (100), (002), (101) (102) (110), (103) and (112) crystal plane respectively. Nearly result of peak positions and identification have been found in other reports that enrich the current results of the proposed study (11,26). According to Scherrer's formula, the X-ray diffraction pattern of ZnO nanoparticles shows an average crystal size of 18.4nm, which in good agreement with other findings is about 20 nm (4).

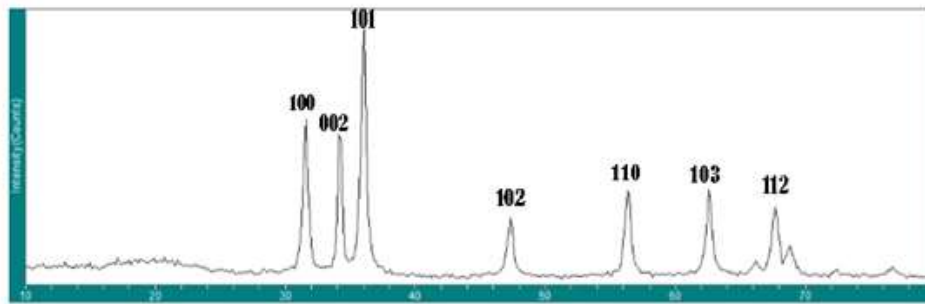


**Figure 10. XRD Patterns of ZnONPs Synthesis by Chemical method**

### (AFM)Atomic Force Microscope

This study investigated surface roughness, topography, and morphology using the technique of atomic force microscopy (AFM). This method provides both 2D and 3D images of the desired nanoparticles at the atomic level. Figure(11) reveals AFM images for three dimensional (3D), 2D images, and particle size distribution of the ZnO. It should be noted that the average diameter of the scanned nanoparticles was estimated at the

nanoscale; where the average diameter of ZnO was (17.03nm), chemosynthesized ZnO nanoparticles were studied by AFM. The surface analysis requires excellent attention because many factors can affect the results of this analysis, such as pollution. The formation of synthesized ZnONPs was confirmed throughout the transition to off-white. It is worth mentioning that the nanoparticles obtained are spherical with an almost homogeneous arrangement.

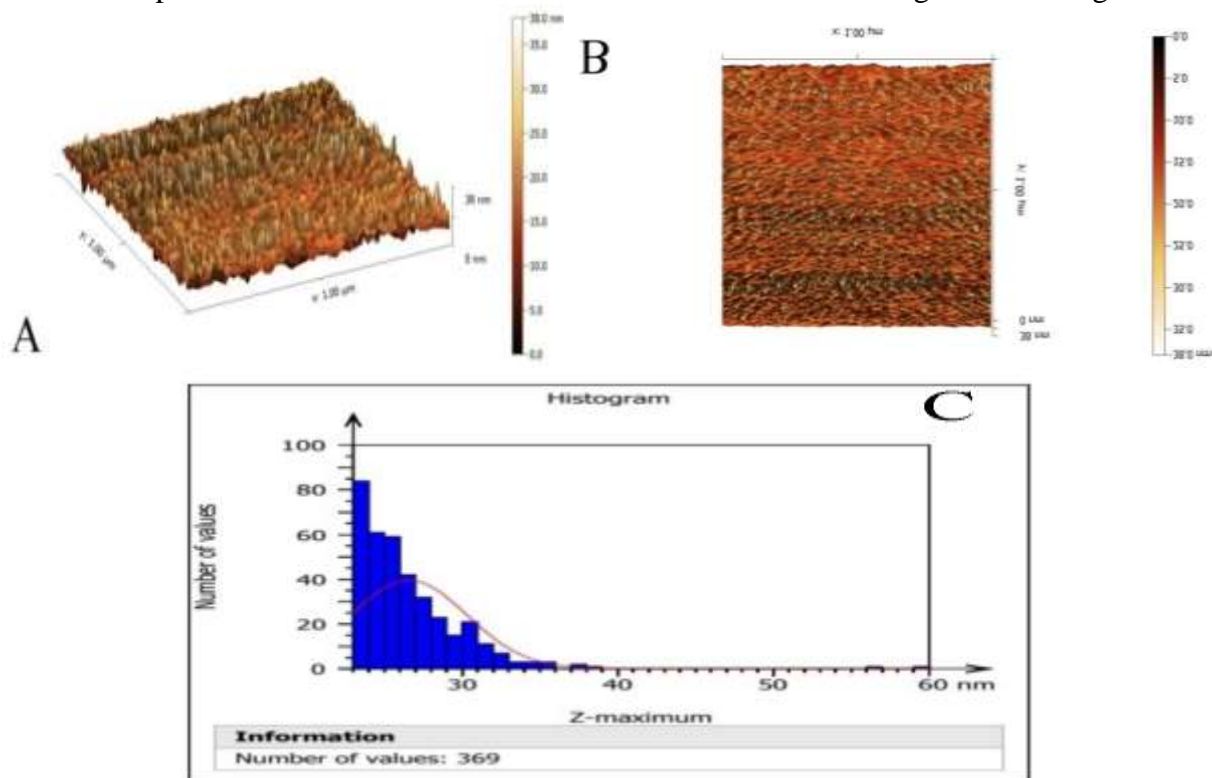


**Figure 11. AFM for ZnO nanoparticles synthesized by the chemical method: (A)3D image (B)2D image (C) Particle size distribution of ZnO nanoparticles**

### E. Zeta Potential measurement

Zeta potential analysis has been done for zinc oxide nanoparticles and ZnO NPs-L-ASNase conjugate at a concentration of 25 $\mu$ g. The analysis shows that the ZnONPS-L-ASNase conjugate at concentration 25 $\mu$ g that revealed the Figure (12) is more stable, having a high

value -23.9 mV of zeta potential compared to ZnO NPs that have -6.1mV value of zeta potential as shows in figure (13-A). Since the value of Zeta potential is increasing, it concluded that the nanoparticles prevent aggregation of protein molecules, increasing their stability.

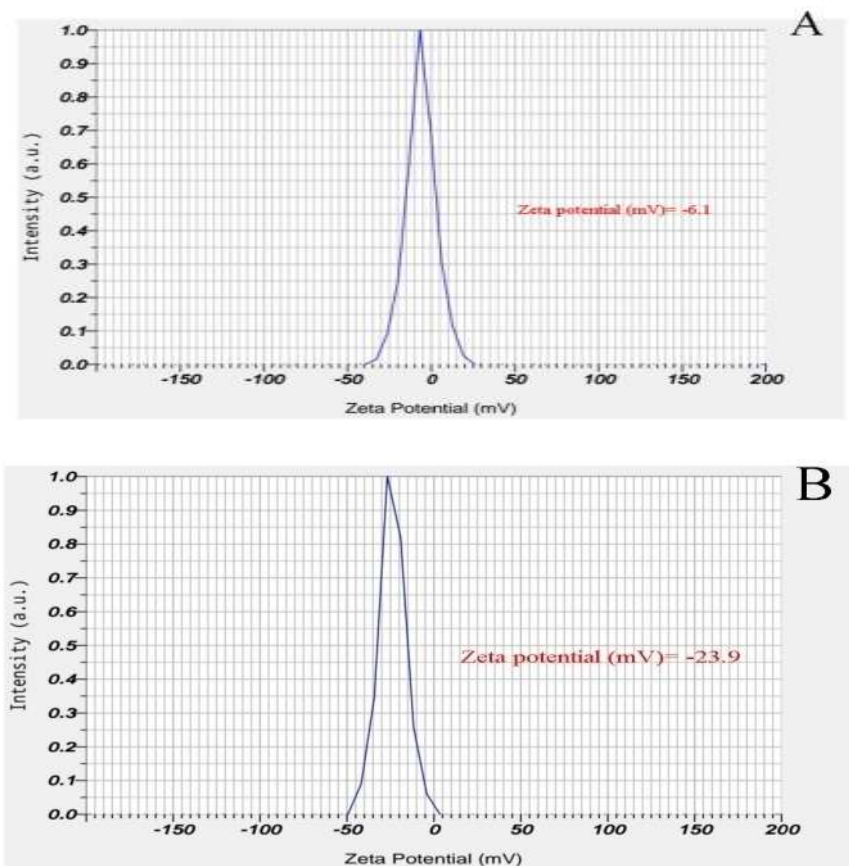


**Figure 12. Zeta Potential measurement (A) Zeta Potential measurement for ZnONPs.(B) Zeta Potential measurement for ZnO NPs-L-ASNase conjugate at concentration 25µg**

#### **Cytotoxic effect on tumor cell lines**

The cytotoxic effect of ZnONPs, LASNase, and the ZnONPs-L-ASNase combination on the tumor (A375 cell) and normal cell lines (WRL68) was determined using the MTT assay. Various concentrations of ZnONPs, L-ASNase and ZnONPs-L-ASNase ranging from 25 to 400 µg mL<sup>-1</sup> for 24 hours were used to measure cell viability in A375 cells and WRL68 cell lines. It has been shown that ZnONPs has a dose-dependent effect on the viability of A375 cells and WRL68 cell lines, as illustrated by Figure (13). At a concentration of 400µg/ mL, the cell viability was 49.5 and 62.6% for A375 cells and WRL68, respectively. Furthermore, the L-ASNase also has a dose dependent effect, the cell viability was 54.7% and 70.8% for A375 cells and WRL68, respectively. On the other

hand, treatment with ZnONPs-L-ASNase showed significant viability in concentrations of 25, 50, 100, 200 and 400 µg mL<sup>-1</sup> with respect to the viability of A375 cells compared to ZnONPs and L-ASNase. IC<sub>50</sub> values of L-ASNase, ZnONPs and ZnONPs-L-ASNase, were about 140.0, 166.5 and 44.69 µg mL<sup>-1</sup>, respectively. On the other hand, all compounds revealed low and moderate cytotoxicity against normal cell lines (WRL-68). Cell viability (%) at a concentration 400 µg mL<sup>-1</sup> remained at 70.8%, 62.6% and 68.2% after treatment with L-ASNase, ZnONPs and ZnONPs-L-ASNase, respectively. WRL-68 does not show any significant differences in the viability pattern of cells at lower concentrations 100 µg mL<sup>-1</sup> and for all treatments.

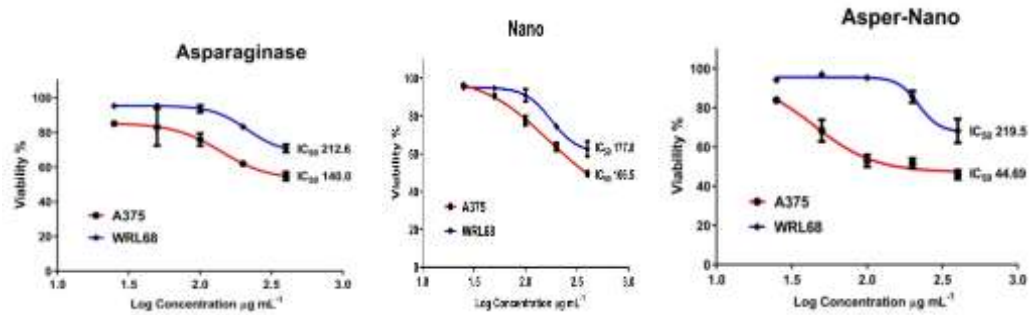


**Figure 13. Cytotoxic effect of L-ASNase, ZnONPs and conjugate (ZnONPs-L-ASNase) against A375 cells and WRL86 cells after 24 hours incubation at 37°C. \*: p value ≤ 0.05- significant**

### Conclusion

*E.coli* was employed to synthesize L-asparaginase metalloproteins coupled to zinc oxide nanoparticles for skin cancer therapy. UV-visible spectroscopy, XRD measurement were used to confirm the production of crystalline metal nanoparticles and metalloproteins. The diameter of synthesized spherical metalloproteins was determined to be 18 nm, AFM used to study investigated surface roughness, topography, and morphology it determined 17.03nm. The reduction in cell survival of A375 cell lines after medication with the metalloprotein demonstrates that the produced metalloproteins possess anti-malignant properties. It was discovered that nanoparticles containing asparaginase are more selective, extremely effective, and produce consistent results.

### REFERENCES

1. Abbas, A. M., S. A., Hammad, H., Sallam, L., Mahfouz A, M. K., Ahmed, S. M., Abboudy, A. E., Ahmed, S. K., Alhag, M. A. Taher, and S. A. Alrumman L, 2021. Biosynthesis of zinc oxide nanoparticles using leaf extract of prosopis juliflora as potential photocatalyst for the treatment of paper mill effluent. *Applied Sciences*, 11, 11394. <https://doi.org/10.3390/app112311394>
2. Abdel Hameed, A. 2005. Production and Characterization of L-Asparaginase from local isolate of *Serratia marcescens* bacteria'. M. Sc. Thesis, Collage of Science, Baghdad University. Iraq. <https://doi.org/10.36103/ijas.v53i6.1668>
3. Ahmed, N., S. S. Mahmood, and A. H. Abbas. 2019. A comparative study of some virulence factors and phylogenetic characterization of *Escherichia.coli* isolates causing urinary tract infection and the

commensal gut. *Iraqi Journal of Agricultural Sciences*, 50(4):1193-1198.

<https://doi.org/10.36103/ijas.v50i4.763>

4. AL-Ariki, S., N. A., Yahya, S. A. A., AL-A'nsi, M. H., Jumali, A. Jannah, and R. Abd-Shukor, 2021. Synthesis and comparative study on the structural and optical properties of ZnO doped with Ni and Ag nano powders fabricated by sol gel technique. *Scientific Reports*, 11, 11948. DOI: [10.1038/s41598-021-91439-1](https://doi.org/10.1038/s41598-021-91439-1)

- 5- Alaa Alden, M. A. and L. A. Yaaqoob. 2022. Evaluation of the biological effect synthesized zinc oxide nanoparticles on *Pseudomonas aeruginosa*. *Iraqi Journal of Agricultural Sciences*, 53(1):.27-37.

<https://doi.org/10.36103/ijas.v53i1.1502>

6. Auda. J. M and M. I. Khalifa. 2019. Cloning and expression of a lipase gene from *Pseudomonas aeruginosa* into *E.coli*. *Iraqi Journal of Agricultural Sciences*, 50(3):768-775. <https://doi.org/10.36103/ijas.v50i3.693>

7. Bradford, M. M. 1976. A rapid and sensitive method for the quantitation of microgram quantities of protein utilizing the principle of protein-dye binding. *Analytical biochemistry*, 72, 248-254. DOI: [10.1006/abio.1976.9999](https://doi.org/10.1006/abio.1976.9999)

- 8- Chagas, E. P. and L. Sodek, 2001. Purification and properties of asparaginase from the testa of immature seeds of pea (*Pisum sativum* L.). *Brazilian Archives of Biology and Technology*, 44, 239-245.

DOI: [10.1590/S1516-89132001000300004](https://doi.org/10.1590/S1516-89132001000300004)

- 9- DIVYA, M., B., Vasearan, M., Abinaya, S., Vijayakumar, M., Govindarajan, N. S., Alharbi, S., Kadaikunnan, J. M. Khaled, and G. Benelli, 2018b. Biopolymer gelatin-coated zinc oxide nanoparticles showed high antibacterial, antibiofilm and anti-angiogenic activity. *Journal of Photochemistry and Photobiology B: Biology*, 178, 211-218.

<https://doi.org/10.1016/j.jphotobiol.2017.11.008>

10- EL-Naggar, N. E.-A. and N. M. El-shweihy, 2020. Bioprocess development for L-asparaginase production by *Streptomyces rochei*, purification and in-vitro efficacy against various human carcinoma cell lines. *Scientific reports*, 10, 7942.

DOI: [10.1038/s41598-020-64052-x](https://doi.org/10.1038/s41598-020-64052-x)

11. Elumalai. K, and S. Velmurugan 2015. Green synthesis, characterization and antimicrobial activities of zinc oxide nanoparticles from the leaf extract of *Azadirachta indica* (L.). *Applied Surface Science*, 345, 329-336.

<https://doi.org/10.1016/j.apsusc.2015.03.176>

12. Hassan, T. J. and S.I. Hussein. 2022. Development of bioprocess for production and purification L-Asparaginase from *Staphylococcus aureus*, and In vitro efficacy against human breast cancer cell line. *Iraqi Journal of Agricultural Sciences*, 53(6):1525-1538. <https://doi.org/10.36103/ijas.v53i6.1668>

13. Hatamzadeh, S., K. Rahnama, S. Nasrollahnejad, K. B. Fotouhifar, K. Hemmati, J. F. White, and F. Taliei. 2020. Isolation and identification of L-asparaginase producing endophytic fungi from the Asteraceae family plant species of Iran. *Peer J* 8 e8309 DOI: [10.7717/peerj.8309](https://doi.org/10.7717/peerj.8309)

14- Imada, A., S., Igarasi, K. Nakahama, and M. Isono, 1973. Asparaginase and glutaminase activities of micro-organisms. *J Gen Microbiol*, 76, 85-99.

DOI: [10.1099/00221287-76-1-85](https://doi.org/10.1099/00221287-76-1-85)

15. Jawad, L.Q. and H.A.R.R., Rasheed. 2022. Isolation and Purification of anticancer protein Exotxin A from *Pseudomonas aeruginosa*. *Iraqi Journal of Agricultural Sciences*, 53(1):48-

56. <https://doi.org/10.36103/ijas.v53i1.1507>

16. Jha S. K, D. Pasrija, R. K. Sinha and H. R. Singh 2012. Microbial L-asparaginase: A review on current scenario and future prospects. *Int J Pharm Sci Res* ;3:3076-90. DOI: [http://dx.doi.org/10.13040/IJPSR.0975-8232.3\(9\).3076-90](http://dx.doi.org/10.13040/IJPSR.0975-8232.3(9).3076-90)

17. Krishnapura, P.R., P.D. Belur, and S., Subramanya, 2016. A critical review on properties and applications of microbial l-asparaginases. *Critical reviews in microbiology*, 42(5), pp.720-737.

DOI: [10.3109/1040841X.2015.1022505](https://doi.org/10.3109/1040841X.2015.1022505)

18. Mohammed, Y. J., J. Y. Mustafa and A. R. Abdullah. 2020. Isolation and molecular study of some bacterial urinary tract infections of sheep in basrah proving. *Iraqi Journal of Agricultural Sciences*, 51(3):885-893.

<https://doi.org/10.36103/ijas.v51i3.1043>

19. Mohideen. A. K. S. 2020. Molecular docking study of L-asparaginase from *Vibrio campbellii* in the treatment of acute lymphoblastic leukemia (ALL). *The EuroBiotech Journal* 4 (1): 8-16

DOI: [10.2478/ebtj-2020-0002](https://doi.org/10.2478/ebtj-2020-0002)

20. Mukherjee, J., S. Majumar, and T. Scheper, 2000. Studies on nutritional and oxygen requirements for production of L-asparaginase by *Enterobacter aerogenes*. *Applied Microbiology and Biotechnology*, 53, 180-184. DOI: [10.1007/s002530050006](https://doi.org/10.1007/s002530050006)

21. Mulvey. M. A. 2002. Adhesion and entry of uropathogenic *Escherichia coli*. *Cellular microbiology*, 4: 257-271

<https://doi.org/10.1046/j.14625822.2002.00193.x>

22. Radadiya, A., W., Zhu, A., Coricello, S. Alcaro, and N. G. J. Richards, 2020. Improving the Treatment of Acute Lymphoblastic Leukemia. *Biochemistry*, 59, 3193-3200. doi: [10.1021/acs.biochem.0c00354](https://doi.org/10.1021/acs.biochem.0c00354)

23. Rakh, R., S., Dalvi, B. Musle, and L. Raut, 2017. Production, extraction and characterization of red pigment produced by *Serratia rubidaea* JCM 1240T isolated from soil. *International Journal of Current Microbiology and Applied Sciences*, 6, 143-154. <http://dx.doi.org/10.20546/ijemas.2017.6.01.018>

24. Rasheed, H. A., R. Alsanee, and H. M. Khalfa, 2022. Anticancer Mechanisms of Zoledronic Acid-Based Graphene Oxide Nanoparticles for Prostate Cancer Bone Metastases Treatment. *Iraqi Journal of Science*, 4241-4253.

<https://doi.org/10.24996/ijs.2022.63.10.11>

25. Ren. J, F. He and L. Zhang. 2010. The construction and application of a new PPY-MSPQC for L-asparaginase activity assay. *Sensors and Actuators. J.*, 145: 272-277.

DOI: [10.1016/j.snb.2009.12.006](https://doi.org/10.1016/j.snb.2009.12.006)

26. Salih. E. Y, M. F. M M Z. Sabri, K. Hussein, Sulaiman, S. M. Said, B. Saifullah, and M. B. A. Bashir 2018. Structural, optical and electrical properties of ZnO/ZnAl<sub>2</sub>O<sub>4</sub>

nanocomposites prepared via thermal reduction approach. Journal of Materials Science, 53, 581-590

DOI: [10.1007/s10853-017-1504-9](https://doi.org/10.1007/s10853-017-1504-9)

27. Schmidt H and M. Hensel 2004. Pathogenicity islands in bacterial pathogenesis. Clin Microbiol Rev 17: 14-56

DOI: [10.1128/CMR.17.1.14-56.2004](https://doi.org/10.1128/CMR.17.1.14-56.2004)

28. Shodiyeva, D., M., Bobakandova, M. Annaev, and Tokhirova, J., 2023. Identification and isolation of endophytic fungi producing l-asparaginase in representatives of the asteratcea family. Science and innovation, 2(D2), pp.107-112.

<https://doi.org/10.5281/zenodo.7643932>

29. Strnadová, M., M., Hecker, L., Wölfel, H. Mach, and J. Chaloupka, 1991. Temperature shifts and sporulation of *Bacillus megaterium*. Microbiology, 137, 787-795

<https://doi.org/10.1099/00221287-137-4-787>

30. Verma. N, K. Kumar, G. Kaur and S. Anand 2007. L-asparaginase: A promising chemotherapeutic agent. Crit Rev Biotechnol;27:45-62.

DOI: [10.1080/07388550601173926](https://doi.org/10.1080/07388550601173926)

31. Warangkar. S. C and C. N. Khobragade 2010. Purification, characterization, and effect of thiol compounds on activity of the *Erwinia carotovora* L-asparaginase. Enzyme Res;1:1-10. doi: [10.4061/2010/165878](https://doi.org/10.4061/2010/165878)

32. Whitaker, J.R. 1994. Principles of Enzymology for the Food Sciences (2nd ed.). Routledge.

<https://doi.org/10.1201/9780203742136>